0026-895X/10/7706-940–952$20.00
MOLECULAR PHARMACOLOGY
Vol. 77, No. 6
63511/3588625
Mol Pharmacol 77:940–952, 2010
Printed in U.S.A.

Pharmacochaperoning of the A_1 Adenosine Receptor Is Contingent on the Endoplasmic Reticulum[S]

Laura Málaga-Diéguez, Qiong Yang, Jan Bauer, Halyna Pankevych, Michael Freissmuth, and Christian Nanoff

Institute of Pharmacology, Center of Physiology and Pharmacology (L.M.-D., Q.Y., H.P., M.F., C.N.) and Center of Brain Research (J.B.), Medizinische Universität Wien, Wien, Austria

Received January 7, 2010; accepted March 9, 2010

ABSTRACT

Exchanging each of the conserved aromatic residues of the NPxxY(x)$_{5,6}$F sequence (at the boundary of helices 7 and 8) generated variants of the A_1 adenosine receptor that were retained within the cell. The mutations disconnected a link between α-helix 7 and cytosolic helix 8, likely destabilizing the structure of the proximal carboxyl terminus. The mutant receptors were rescued by incubation of cells with a pharmacochaperone, a membrane-permeable ligand that homosterically binds to the receptor; pharmacochaperoning restored the density of functional receptors at the plasma membrane. The following observations support the assumption that retention and the site of pharmacochaperone action were within bounds of the endoplasmic reticulum (ER): 1) the retained receptor colocalized with an ER marker; 2) pharmacochaperoning initiated receptor transfer to Golgi stacks; and 3) the inhibitor of glycoprotein synthesis tunicamycin suppressed receptor chaperoning. Our data are consistent with the hypothesis that pharmacochaperoning stabilizes the structure of late folding intermediates and lifts a block on maturation, allowing the receptors to exit from the ER. We suggest that the ER-associated 40-kDa heat shock protein family member D_1 receptor interacting protein 78 (DRiP78; M_r, ~78,000) represents a model executor of quality control. Overexpressed DRiP78 interacted physically with the A_1 receptor, inhibited export to the plasma membrane, and in this action was selective for the mutants relative to the wild-type receptor. Both agonist and antagonist were effective chaperone ligands. Thus, occupancy of the binding pocket corrected the mutation-induced disorder, indicating a mutual impingement of the transmembrane domain and the proximal carboxyl terminus in establishing the stable receptor fold.

G protein-coupled receptors are glycosylated integral membrane proteins localized at the cell surface. At any time, their density on the cell surface is the result of receptor trafficking to and sequestration away from the plasma membrane. Delivery to the cell surface is caused by recycling of internalized receptors, or it follows export of newly synthesized receptors. Up-regulation of functional receptors caused by receptor-specific ligands may be caused by diminished internalization or accelerated export. The concept of pharmacochaperoning refers to the latter (Morello et al., 2000).

Chaperone ligands (pharmacochaperones) have been found to deliver retained receptors to the cell surface and afford functional rescue (Chaipatikul et al., 2003; Noorwez et al., 2003; Wüller et al., 2004; Fan et al., 2005; Robert et al., 2005b; Hawtin, 2006). It is a consistent requirement that ligands can penetrate into the cell; the pharmacochaperone effect is concentration-dependent in a range commensurate with the affinity value of the surface-exposed receptor. Retention in the endoplasmic reticulum (ER) or a later compartment along the secretory pathway means that the receptor has not acquired the proper native conformation. Pharmacochaperones therefore must act to bypass the local quality-control system.

This work was supported by the Austrian Science Fund [Grants 16083-B11, P18150-B11].
Article, publication date, and citation information can be found at http://molpharm.aspetjournals.org.
doi:10.1124/mol.110.063511.
[S] The online version of this article (available at http://molpharm.aspetjournals.org) contains supplemental material.

ABBREVIATIONS: ER, endoplasmic reticulum; CPA, N^6-cyclopentyladenosine; DPCPX, 8-cyclopentyl-1,3-dipropylxanthine; IBMX, 3-isobutyl-1-methylxanthine; DRiP78, D_1-receptor-interacting protein 78; A_1R, A_1 adenosine receptor; C-tail, cytoplasmic carboxyl-terminal tail; wt, wild type; HA, hemagglutinin; CFP, cyan fluorescent protein; ECFP, enhanced CFP; YFP, yellow fluorescent protein; GFP, green fluorescent protein; HEK, human embryonic kidney; IP, immunoprecipitation; PDI, protein disulfide isomerase; ICQ, intensity correlation quotient; HME, HEPES/$MgCl_2$/EDTA; HRP, horseradish peroxidase; DSP, dithiobis[succinimidylpropionate]; CHAPS, 3-[(3-cholamidopropyl)dimethylammonio]-1-propanesulfonic acid; BFA, brefeldin A; Hsp, heat shock protein.

In judging the integrity of the folding products, the quality-control system follows its own specific rules. It is a repeated observation that proteins are retained despite only minimal alterations in structure. Likewise, G protein-coupled receptors are retained because of single-point mutations (Noorwez et al., 2003; Mizrachi and Segaloff, 2004; Fan et al., 2005; Hawtin, 2006). These may give rise to misfolding of a particular subdomain (cytosolic, membranous, luminal). Because subdomains are probed separately, retention and sorting to ER-associated degradation can be the consequence of single-point mutations (Huyer et al., 2004).

Single amino acid substitutions that lead to the retention of G protein-coupled receptors have been found mostly scattered along the transmembrane domain (Mizrachi and Segaloff, 2004; Fan et al., 2005; Conn et al., 2006; Hawtin, 2006). Although vulnerable, the transmembrane domain is considered to have the highest thermodynamic stability because of a number of interhelical noncovalent bonds. Accordingly, the arrangement of the seven-transmembrane α-helices in rhodopsin and the β_2 adrenergic receptor crystal structures is very similar (Cherezov et al., 2007). By contrast, the extracellular and intracellular segments differ between rhodopsin and the β_2 receptor.

The only other secondary structure present and superimposable in the rhodopsin and β_2 adrenergic receptor crystal structures is helix 8 of the membrane-proximal C-tail. Helix 8 projects at a sharp angle from the cytoplasmic end of the seventh transmembrane α-helix. The available structural information indicates that the membrane-proximal C-tail is stabilized by a stacked interaction between the aromatic rings of tyrosine (within the transmembrane helix VII) and phenylalanine (within the C-tail) that belong to the conserved NPxxY$(x)_{5,6}$F sequence. Thus, the transmembrane domain impinges on folding of the proximal C-tail, and helix 8 seems to be a constant feature when the receptor folds. Conversely, lesions to helix 8 lead to receptor retention; indeed, receptors with deletions/mutations in the proximal C-tail are notorious for not being exported to the cell surface (Gáborik et al., 1998; Oksche et al., 1998; Bermak et al., 2001; Chaipatikul et al., 2003; Pankevych et al., 2003; Duvernay et al., 2004; Robert et al., 2005a; Thielen et al., 2005; Sawyer et al., 2010).

We have used the A_1 adenosine receptor to examine the conditions necessary for efficient pharmacochaperoning. We had shown previously that the A_1 receptor with a close C-terminal truncation gave a low surface level and was retained mostly in the ER (Pankevych et al., 2003); the truncated receptor responded to pharmacochaperoning (Hawtin, 2006). A major experimental advantage in using the A_1 receptor is that it is largely excluded from dynamic receptor trafficking; receptor density on the cell surface is determined by the equilibrium between export of newly synthesized receptors and their degradation with little interference from receptor recycling (Klinger et al., 2002). By mutating the stabilizing aromatic residues out of the NPxxY$(x)_{5,6}$F sequence, our present data support the hypothesis that folding of helix 8 is necessary for receptor export. The mutant receptors, as opposed to the wild type, exhibited marked up-regulation in response to a chaperone ligand. In addition, our findings are compatible with the assumption that pharmacochaperoning releases receptor association to an ER-resident chaperone protein.

Materials and Methods

Materials. The rat A_1 receptor (A_1R) (wild-type receptor) extended on the N terminus with a hemagglutinin (HA)-epitope tag was expressed in mammalian cells by using the vector and the transfection method as described (Pankevych et al., 2003); stable cell lines were raised by selecting for G-418 (Geneticin) resistance. An expression vector for the A_1 adenosine receptor tagged at the carboxyl-terminal end with enhanced yellow fluorescent protein (and with the FLAG epitope on the N terminus, A_1R-YFP) was a gift from Dr. R. Franco (University of Barcelona, Barcelona, Spain). Point mutations Y288A and F295A and a double mutation (Y288A and F295A) were introduced into the coding sequence of the wild-type receptor by using the QuikChange II mutagenesis kit (Stratagene, La Jolla, CA); the Y288A mutation was introduced into A_1R-YFP.

The bacterial expression vector encoding the human A_1-receptor (pMES-A_1) has been described by Jockers et al. (1994). Tyrosine at position 288 was mutated to alanine to give the Y288A receptor variant for expression in *Escherichia coli* (pMES-A_1 Y/A).

The following expression vectors were kindly donated: for the β_2-adrenergic receptor by Dr. Blanche Schwappach (University of Heidelberg, Heidelberg, Germany) and for Sar1A[T39N] by Dr. H. Farhan (Medizinische Universität Wien, Wien, Austria). Sar1A[T39N] is the GDP-trapped, inactive form of Sar1A that acts in a dominant negative manner to suppress vesicle budding from the ER membranes (Kuge et al., 1994). An expression vector for DRiP78 (rat ortholog) was donated by Dr. Q.-Y. Zhou (University of California, Irvine, CA); full-length DRiP78 was cloned into the ECFP-N1 vector (Clontech, Mountain View, CA) for mammalian expression of DRiP78 fused on its C terminus to CFP.

The pECFP-ER vector and the pECFP-Golgi vector (Clontech) were used to visualize the ER and the medial-trans region of the Golgi apparatus, respectively.

Plasmids were purified with kits from QIAGEN (Valencia, CA). Oligonucleotides were obtained from GenXpress (Maria Wörth, Austria) and Operon (Cologne, Germany); the integrity of the DNA constructs used was verified by fluorescent sequencing. For receptor expression in *E. coli* the Rosetta strain of BL21(DE3) bacteria was used. Expression of the A_1 receptor in bacteria and the preparation of bacterial membranes were done as described previously (Jockers et al., 1994).

Radiochemicals were obtained from PerkinElmer Life and Analytical Sciences (Waltham, MA). Restriction enzymes were from Fermentas (Ontario, Canada), and adenine and guanine nucleotides were from Roche Molecular Biochemicals (Indianapolis, IN). Antibodies detecting the HA and FLAG epitopes (M2) were from Sigma-Aldrich (St. Louis, MO), the anti-GFP antibody that cross-reacts with CFP and YFP was from Clontech, and the polyclonal anti-protein disulfide isomerase (PDI) antibody was from Stressgen Biotechnologies. The secondary horseradish peroxidase (HRP)-conjugated antibodies were from GE Healthcare (Chalfont St. Giles, Buckinghamshire, UK). HRP substrates were from Thermo Fisher Scientific (Waltham, MA). Cell culture media and supplements were from PAA Industries (Linz, Austria). All other chemicals and reagents were of the highest purity grade available.

Antibody Staining of HEK293 Cells Expressing the A_1 Receptor. Human embryonic kidney cells (HEK) 293 cells were seeded onto coverslips coated with poly-D-lysine and transfected with HA-tagged A_1-receptor variants by using the LipoPlus transfection reagent (Invitrogen). For cotransfection the total amount of DNA was kept constant by using, if necessary, the empty pcDNA3 vector (Invitrogen).

Antibody staining of the receptor in fixed cells was carried out as described previously (Pankevych et al., 2003), except cells had been transiently transfected and were permeabilized with 0.2% Triton X-100 in phosphate-buffered saline (20 min at room temperature). Staining was carried out with a monoclonal mouse anti-HA (16B12) antibody (Covance Research Products, Princeton, NJ) and a second-

ary Alexa Fluor 488-conjugated goat anti-mouse IgG (Invitrogen). Confocal microscopy was performed under oil immersion with a laser scan microscope (Zeiss LSM 510; Carl Zeiss GmbH, Jena, Germany).

Live Cell Microscopy. Confocal microscopy was carried out at room temperature by using transiently transfected HEK293 cells. The fluorescence of YFP or CFP was captured sequentially by using the 458- and 514-nm line of the argon laser for CFP and YFP, respectively, and a 458/514-nm beam splitter. CFP emission was detected with a bandpass 475- to 525-nm filter, and YFP emission was detected with a long-pass 530-nm filter. Images were averaged from four scans. For CFP and YFP colocalization, images were captured by using both lines of the argon laser simultaneously. Fluorescence images were background-corrected and merged with MetaFluor (Molecular Devices, Sunnyvale, CA) or Wright ImageJ software (Wright Cell Imaging Facility, Toronto, ON, Canada). The confocal microscopes used were from Carl Zeiss GmbH or Leica (Wetzlar, Germany).

Intensity Correlation Analysis. To assess and quantify colocalization of compartment markers (ER-CFP, Golgi-CFP) and the mutant A_1 receptor, an intensity correlation analysis was performed. The analysis was done as described previously (Li et al., 2004) by using an applet of Wright ImageJ software. Confocal images of cells cotransfected with A_1R Y288A-YFP and compartment markers, specifically the area outlined by the marker (ER or Golgi), were subjected to analysis. Positive pixel values indicated that receptor distribution was dependent of the compartment marker. For each image the number of pixels that generated positive values was counted; the ratio of positive values over the total number of pixel pairs reflected the degree of colocalization. An intensity correlation quotient (ICQ) was generated by subtracting 0.5 from this value.

Fractionation by Sucrose Density Gradient Centrifugation. Fractionation of a postnuclear homogenate of HEK293 cells was carried out as described previously (Pankevych et al., 2003). In brief, HEK293 cells were collected by centrifugation, taken up in hypotonic HME buffer (25 mM HEPES·NaOH, pH 7.5, 2 mM $MgCl_2$, and 1 mM EDTA) including protease inhibitors (Roche Diagnostics, Indianapolis, IN), and disrupted by a freeze-thaw cycle. Cells were further homogenized with a glass pestle homogenizer (five strokes). The nuclear fraction was settled by low-speed centrifugation (15 min at 1000*g*, 4°C) and discarded. The postnuclear supernatant (1.0–2.5 mg of protein) was mixed with sucrose to give a concentration of 40% in 3-ml volume, layered on the bottom of a 36-ml centrifugation tube (Beckman Coulter, Fullerton, CA). We generated sucrose gradients by sequentially adding 11 3-ml cushions of sucrose (range, 16 to 38%) in HME buffer. For the resolution of plasma membrane fractions (~1.06–1.13 g/ml specific gravity), the sucrose cushions covered a concentration range of 16 to 32%; to separate light and heavy membranes the concentration range was between 18 and 40% (~1.07–1.15 g/ml). Membranes were brought to their isopycnic flotation density by centrifugation for 16 h at ~100,000*g*. Fractions were collected by aspiration from the top and screened for protein content, the A_1 receptor, Na^+/K^+-ATPase, and PDI.

Immunoprecipitation of the A_1 Receptor. Receptor immunoprecipitation (IP) was carried out as described previously (Pankevych et al., 2003), except membranes from a stable cell line expressing the Y288A receptor mutant [3 mg corresponding to a [^{3}H]8-cyclopentyl-1,3-dipropylxanthine (DPCPX) binding level of 30 fmol/mg] were used. For IP a monoclonal anti-HA antibody was used (clone HA-7; Sigma-Aldrich), for developing the immunoblot a polyclonal antibody (Y-11; Santa Cruz Biotechnology, Inc., Santa Cruz, CA). To enhance reactivity in some instances we used a mix of polyclonal and monoclonal antibodies. To visualize the position of the secondary antibodies we used a highly sensitive HRP substrate (Thermo Fisher Scientific). For co-IP, a cell line expressing the mutant A_1 receptor (Y288A) was transfected with CFP-tagged DRiP78. Cell membranes (4 mg) were cross-linked by incubation with 2 mM dithiobis[succinimidylpropionate] (DSP; Thermo Fisher Scientific) in a volume of 1 ml, according to the manufacturer's instructions. Cross-linked membranes were solubilized in detergent buffer (10 mM CHAPS, 150 mM NaCl, 0.1 mM phenylmethylsulfonyl fluoride in HME). After clearing the soluble supernatant, receptor was precipitated (without reducing the detergent concentration) with the monoclonal anti-HA antibody, separated on an SDS-urea gel, and transferred to nitrocellulose. The immunoblot was developed with a polyclonal anti-HA antibody and an anti-CFP antibody (Clontech).

Miscellaneous Procedures. Cell culture, preparation of cell membranes, radioligand binding, and measurement of cellular cAMP formation were carried out as described previously (Pankevych et al., 2003). Clonal cell lines expressing the A_1 adenosine receptor (wild type and mutants) were raised after transfection by selecting for G418 resistance.

To eliminate carryover of residual amounts of chaperone ligand, membranes were washed extensively during preparation. To control that the membranes were void of unlabeled ligand [^{3}H]DPCPX saturation isotherms were examined for radioligand affinity (not shown). Only with DPCPX (used as chaperone ligand) did pretreatment result in a right shift of the saturation curve (by a factor of two) in some preparations. Thus, the effect size of DPCPX may have been underestimated when determined by a single fixed concentration of [^{3}H]DPCPX.

Radioligand binding to intact bacterial cells was carried out in a final volume of 100 μl, 40 μl of which was *E. coli* suspension. After inducing receptor expression, bacteria (70-ml culture volume; optical density, ~1) were resuspended in 2 ml of phosphate-buffered saline and immediately dispensed to the reaction tubes. [^{3}H]DPCPX binding was added at various concentrations in the presence of adenosine deaminase (1 U/ml); incubation was for 1 h at 30°C. Nonspecific binding was defined with xanthine amine congener (1 μM) and amounted to 50% in the K_D concentration range. Statistical analysis was performed by using a commercial program (Analyze-It Software, Ltd., Leeds, UK).

Results

Mutagenesis Directed at Destabilizing Helix 8 Causes Intracellular Retention of A_1 Receptors. In the A_1 adenosine receptor, the proximal C-tail probably forms an amphipathic helix (Pankevych et al., 2003). Mutating the tyrosine of the NPxxY sequence or the phenylalanine of helix 8 (which are separated by six residues) to alanine decreased cell surface expression of the receptor. We used antibody staining in permeabilized cells and radioligand binding ([^{3}H]DPCPX at a saturating concentration of ~10 nM) to assess the receptor density in transiently transfected HEK293 cells. Figure 1A shows that with the mutant receptors (Y288A, F295A) binding was only 4 to 5% of wild type. Antibody staining of the epitope tag in permeabilized cells revealed receptor accumulation within the cell interior (Fig. 1C, top) but did not label the cell surface (including the typical plasma membrane extensions with which the cells attach to the coated-glass support); staining of the wild-type receptor by contrast lined the cell surface (Fig. 1C, top right). Live-cell imaging (Fig. 1C) of the YFP-tagged receptor confirmed the effect of the single-point mutation (Y288A).

Mutant Receptors Are Exported after Incubation of Cells with a Receptor Ligand. Cell incubation with a receptor-specific ligand greatly restored surface expression. We first tested ligands with antagonist/inverse agonist properties. Of the ligands tested, the methylxanthines DPCPX and 3-isobutyl-1-methylxanthine (IBMX) and the agonist N^6-cyclopentyladenosine (CPA) have lipophilic substituents that allow for uptake independently of specific transporters

(Plagemann and Wohlhueter, 1984). The ligand concentrations used were close to a saturating concentration for cell surface-bound receptors (50 μM for IBMX; 1 μM for DPCPX).

Figure 1, A and B, demonstrates the effect of the antagonists (DPCPX, ▧; IBMX, ▩) on the receptor binding level. Both DPCPX and IBMX increased radioligand binding to the mutant receptors, whereas the effect on the wild-type receptor was barely measurable (Fig. 1B). The increase was similar when the YFP-tagged version of the Y288A mutant was used (not shown). Accordingly, cells transfected with either the Y288A or the F295A mutant that had been treated with DPCPX exposed the receptors on the cell surface. Antibody staining lined the plasma membrane and its extensions, whereas the cell interior was, in many instances, void of immunoreactivity (Fig. 1C). The change in receptor distribution is exemplified clearly with the mutant YFP-tagged version (Fig. 1C).

Single-Site Mutant A_1 Receptors Are Functionally Intact but Differ in G Protein Coupling. We tested the ability of the mutant receptors to signal in response to an agonist by assessing the inhibition of cAMP formation. Because mutations in the helix 8 region and the conserved $NPxxY(x)_{5,6}F$ motif can impair G protein coupling (Prioleau et al., 2002; Fritze et al., 2003; Delos Santos et al., 2006), we also examined whether the mutant receptors adopt the high-affinity agonist-bound conformation that is representative of agonist-mediated G protein activation.

Fig. 2 shows the effect of CPA on cells pretreated (Fig. 2B) or not (Fig. 2A) with a chaperone ligand. In untreated cells, the Y288A mutant failed to inhibit cAMP formation, whereas A_1R F295A did; the latter was indistinguishable from wild type. In contrast, A_1R Y288A mediated inhibition only after preincubation with the chaperone ligand. Subsequently, maximal inhibition and the apparent potency of CPA were similar for the Y288A (44% of maximum, 84 nM) and the F295A mutant (49%, 114 nM); both resembled wild type.

The inability of Y288A to inhibit cAMP formation in untreated cells was caused by a reduced propensity of the agonist-occupied receptor to couple to its cognate G protein, G_i (Supplemental Fig. 1). As opposed to the F295A mutant, a G protein-coupled high-affinity state could not be discerned for the Y288A receptor, accounting for its inability to inhibit cAMP. Even after pretreatment with the chaperone ligand only a few of the Y288A receptors (8 and 13% in two independent experiments) formed the high-affinity state. Thus, the refractoriness of Y288A to adopting the high-affinity conformation was not eliminated by pharmacochaperoning. In the F295A mutant, by contrast, coupling appeared to be

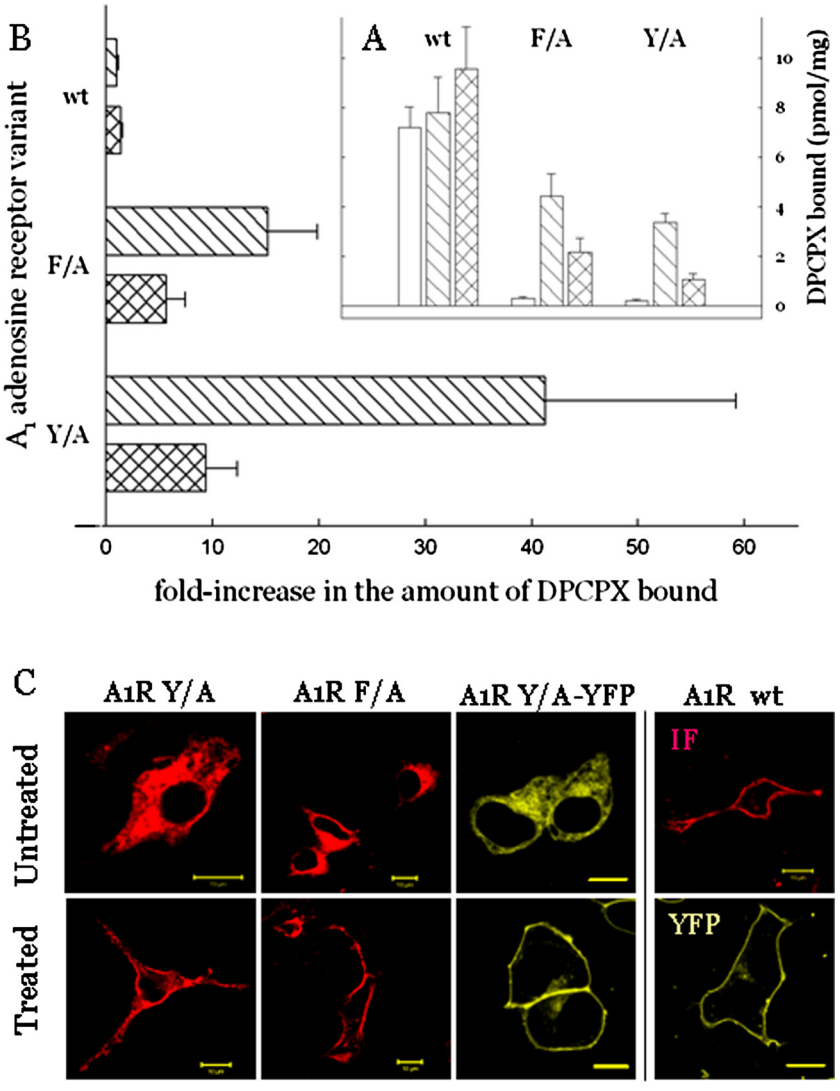

Fig. 1. Intracellular retention and rescue of mutant A_1 adenosine receptors. A, expression level of an A_1 receptor with the wild-type sequence and receptor variants with a point mutation in TM7 (Y288A, Y/A) or the adjacent cytoplasmic sequence (F295A, F/A). Receptor levels were measured by radioligand binding to membrane preparations from cells treated with vehicle (□), 1 μM DPCPX (▧), or 50 μM IBMX (▩). Data are means ± S.E.M. from six to 15 transfection experiments carried out in parallel. [^{3}H]DPCPX binding was performed at a single saturating concentration (approximately 10 nM). B, data from A expressed as ligand-induced increase (fold over basal; error bars, 99% confidence interval). C, visualization of the mutant A_1 receptors before (top) and after (bottom) treatment of cells (for 24 h before fixation) with 1 μM DPCPX. Shown is receptor localization by immunofluorescence (F/A; Y/A; wt, IF) or YFP-tag fluorescence (Y/A-YFP; wt, YFP). Scale bar, 10 μm.

enhanced relative to wild type (compare Pankevych et al., 2003); the F295A receptors that were exported spontaneously (resulting in a density of ~300 fmol/mg on average) apparently sufficed to exert maximal effector regulation.

Antagonist and Agonist Ligands Are Effective in Pharmacochaperoning. We assessed the specificity requirements underlying the chaperone effect. The apparent potencies of DPCPX and IBMX, estimated in a cell line stably expressing the Y288A mutant, differed by approximately four orders of magnitude (Fig. 3A). The difference reflected the respective binding affinities for the wild-type receptor (K_D for IBMX, ~10 μM; K_D for DPCPX, ~1 nM); the EC_{50} for DPCPX, estimated from experiments in three Y288A cell lines, was 15.3 ± 6.8 nM (mean ± S.E.M). The concentration-effect curve for DPCPX, but not the [^{3}H]DPCPX saturation isotherm (not shown), was steeper than unity (Hill coefficient = 1.57 ± 0.36), presumably because at low concentrations free ligand was quenched by being adsorbed to lipid membranes. IBMX even at the highest concentration (250 μM) failed to induce the maximal expression level attained with DPCPX, which accounts for the moderate effect level documented in Fig. 1B. The difference was confirmed in a time course experiment where we followed the pharmacochaperone-induced increase in radioligand binding, up to the average doubling time of HEK293 cells (~24 h; Fig. 3B). With both receptor mutants, Y288A and F295A, the increase was gradual and quasi-linear for either antagonist used. The time course paralleled the surface targeting of a spontaneously exported receptor (Van Craenenbroeck et al., 2005).

In addition, an agonist ligand (CPA) was tested in stable cell lines expressing either of the mutant receptors (Y288A, F295A). The results indicated that incubation with CPA (50 μM) caused an increase in receptor number. We have ruled out that the effect was mediated by the solvent dimethyl sulfoxide, a chemical chaperone (not shown). The effect was indistinguishable from that of DPCPX in size (Fig. 3C, and time course, not shown). The agonist effect was independent of the inserted mutation. Conversely, when the wild-type receptor had been exposed to CPA for 24 h there was no

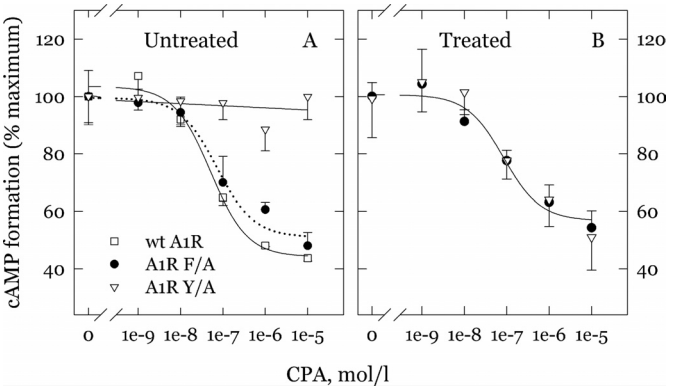

Fig. 2. Mutant A_1 receptors are functional. Inhibition of cAMP formation by the A_1 receptor mutants in transiently transfected cells that had not (A) or had been (B) incubated with a chaperone ligand. Formation of cAMP was determined in cells transfected with an A_1 receptor construct (wt, □; F295A, ●; Y288A, ▽); adenylyl cyclase activity was stimulated with isoprenaline via a cotransfected β_2-adrenergic receptor. Shown are representative experiments performed in triplicate. The values were normalized to the amount of cAMP measured in the absence of CPA. Error bars, S.E.M.

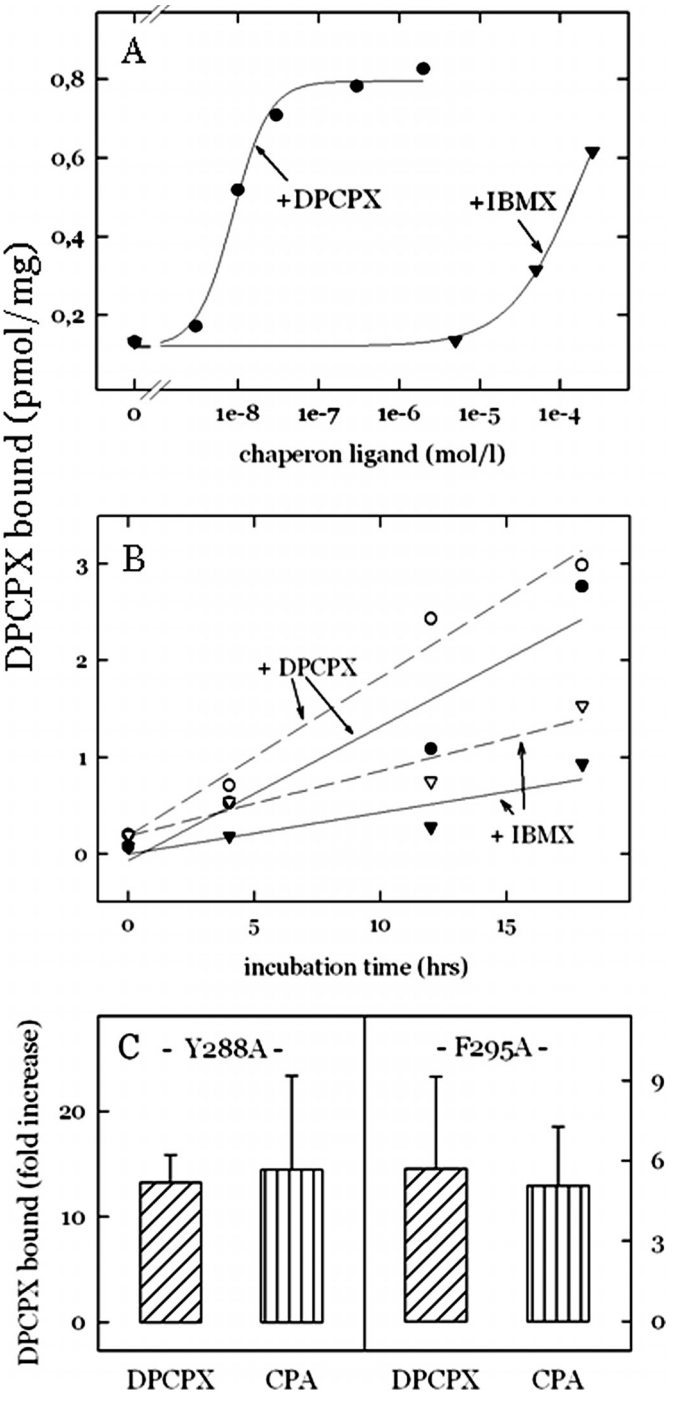

Fig. 3. Homosteric ligand binding to the retained mutant A_1 receptors causes pharmacochaperoning. A, DPCPX or IBMX were added at the indicated concentrations to a HEK293 cell line stably expressing A_1R Y288A. After 24 h the receptor level was assessed by [^{3}H]DPCPX binding to a cell membrane preparation. The data shown are from a representative experiment where each point represents the mean of two separate dishes. The experiment was repeated with two alternative stable cell lines yielding similar results. B, receptor levels were measured by radioligand binding to membranes from cells transiently transfected with A_1R Y288A (●, ▼) or A_1R F295A (○, ▽) at three time points after the addition of DPCPX (●, ○) or IBMX (▽, ▼); the chaperone ligand was added for the indicated incubation periods before harvest (48 h after transfection). The experiment was repeated twice with similar results. C, stable cell lines expressing A_1R Y288A and A_1R F295A were incubated for 24 h, in parallel, with 1 μM DPCPX (▨) or 50 μM CPA (▥), and the receptor level was assessed (as in A). Given are increments (± S.D.) in receptor density, relative to untreated controls, from at least three independent experiments. The experiments were carried on different clonal cell lines.

significant change in receptor number; specifically, receptor down-regulation did not occur (not shown).

The Majority of Ligand-Binding A_1 Receptors Are Localized in the Plasma Membrane. Our data suggested that pharmacochaperoning increased the density of plasma membrane-bound receptors; the mutant receptors arrived at the cell surface (Fig. 1C) and were situated to regulate effector activity (Fig. 2). We directly assessed the receptor distribution after cell fractionation to confirm that the images and the functional effects were representative of the entire population of cells. HEK293 cells transfected with the F295A receptor were incubated in the absence or presence of a chaperone ligand for a day before harvest. A postnuclear cell homogenate was prepared and fractionated on a sucrose density gradient. Figure 4 shows radioligand binding to F295A receptors in the gradient fractions. Receptor distribution was compared with the distribution of Na^+/K^+-ATPase (marker for plasma membranes) and PDI (ER marker). Consistent with the results from binding to unfractionated membranes (Fig. 1), the receptor density increase caused by pharmacochaperoning was large when fractions were compared from untreated (Fig. 4A, *y* axis scale from 0.1 to 1.0 pmol/mg) and treated cells (Fig. 4B, scale from 1 to 70 pmol/mg).

Before and after pharmacochaperoning, receptor and Na^+/K^+-ATPase had a very similar distribution, which peaked in the light fractions. The resulting plots are similar, indicating that the receptor was detected by radioligand binding only in fractions enriched in Na^+/K^+-ATPase. Because the resolu-

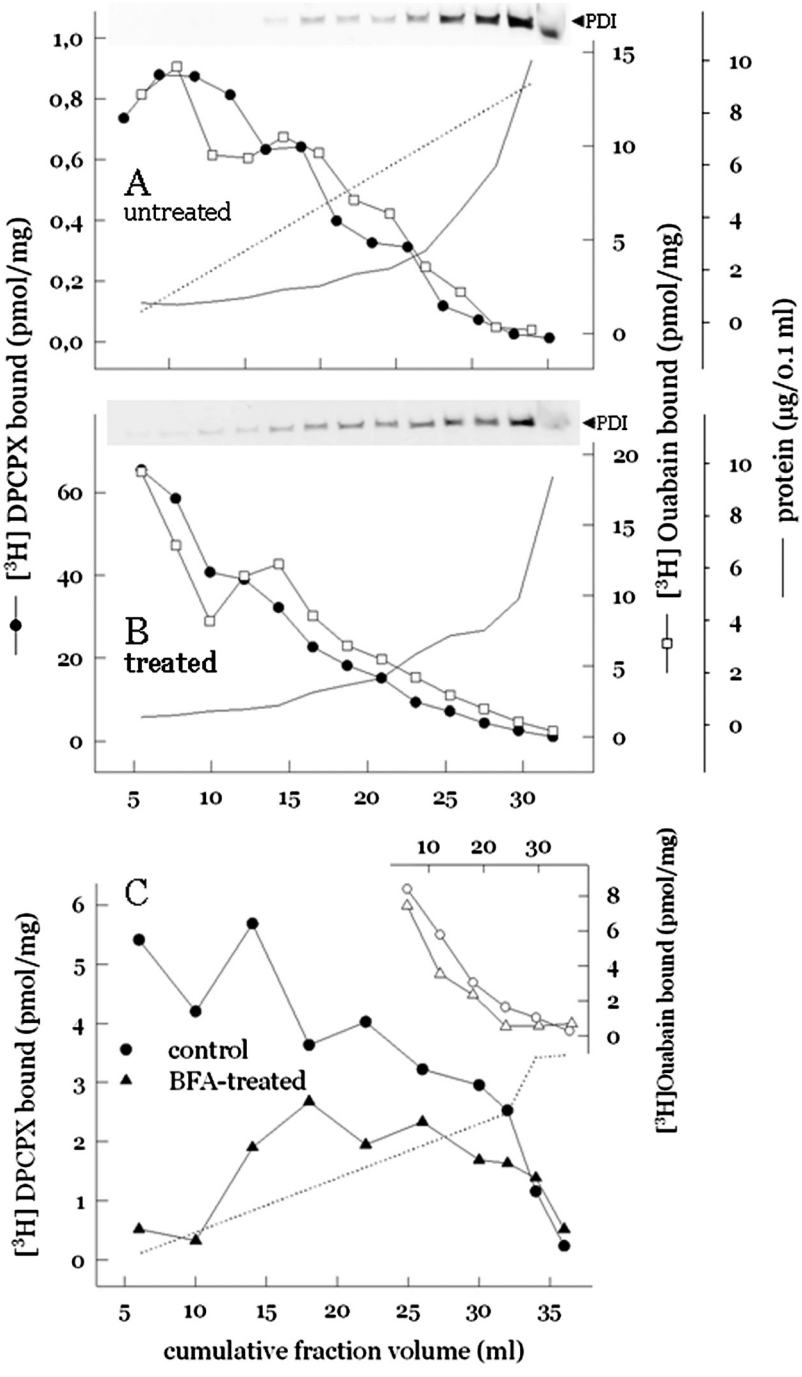

Fig. 4. Fractionation of HEK293 cells expressing A_1R F295A: plasma membrane localization of ligand binding receptors. A and B, a postnuclear supernatant (approximately 1 mg) was prepared from transiently transfected HEK293 cells and applied to a 36-ml discontinuous sucrose gradient. Fractions were analyzed by radioligand binding and immunoblotting. Charted are protein concentration and PDI immunoreactivity; the A_1 receptor (●) and Na^+/K^+-ATPase (○) are expressed as the amount of radioligand specifically bound per milligram of protein to document marker enrichment. Transfected cells had not (A) or had been (B) treated with DPCPX for 24 h before harvest; the *y* axis scales for the amount of DPCPX bound are different in A and B to highlight the similar subcellular distribution. The dotted line in A indicates the calculated fraction density in the range of 1.08 to 1.15 g/ml. C, sucrose gradient fractionation of cells stably expressing A_1R F295A. Cells were incubated for 24 h before harvest with DPCPX and, for the last 5 h, with (▲) or without (●) BFA (5 μg/ml). Specific binding of [^{3}H]DPCPX and [^{3}H]ouabain (inset) is charted; fraction density was between 1.08 to 1.15 g/ml (dotted line). The fractions shown cover the range where Na^+/K^+-ATPase binding activity was enriched (inset).

tion of subcellular fractionation sufficiently separated the peak of Na^+/K^+-ATPase and the ER marker (PDI), the predominant amount of radioligand binding therefore must reflect receptor surface expression.

Pharmacochaperoning Requires Receptor Transit through the Golgi. We further explored the mechanism of pharmacochaperoning presuming that ligand binding accelerated receptor export from the site of biosynthesis to the plasma membrane. Accordingly, pharmacochaperoning should be impaired if transit through the Golgi were interrupted. We used brefeldin A (BFA), which causes a rapid dissociation of Arf1 (ADP-ribosylation factor 1) and coat adaptor proteins from Golgi membranes to block the canonical ER-to-surface transport. HEK293 cells from a stable line expressing the mutant receptor (A1 F295A) were treated with IBMX for 24 h; for the last 6 h before harvest, BFA (5 μg/ml) was added. BFA-treated and nontreated cells were homogenized and fractionated on a shallow sucrose gradient to resolve the plasma membrane (specific density between ~1.08 and 1.13 g/ml); heavier membranes were collected in the bottom fraction (~1.15 g/ml). Specific DPCPX and ouabain binding data are plotted in Fig. 4C.

It is obvious that the A_1 receptor density in the light membrane fractions dropped as a consequence of the BFA-induced block. The binding values were normalized to the protein concentration; unequal cell recovery during harvesting (which was ~50% lower after BFA treatment) therefore could not account for the lower receptor number. Relative to the A_1 receptor, Na^+/K^+-ATPase density was much less affected by BFA (Fig. 4C, inset), reflecting different half-lives (the receptor was shorter lived than endogenous Na^+/K^+-ATPase). Thus, BFA impeded pharmacochaperoning; conversely, receptor recruitment must occur at the ER or a post-ER compartment (e.g., the ER-Golgi-intermediate compartment).

In Bacteria, Chaperone Ligands Do Not Increase the Yield of Properly Folded Receptors. We hypothesized that the chaperone ligand facilitated the folding process (e.g., by supplying a folding nucleus). If so, pharmacochaperoning would up-regulate receptors even when expressed in prokaryotic cells; in bacteria (*E. coli*), expression of membrane proteins results in cotranslational insertion of the polypeptide in the plasma membrane. Because folding of the foreign receptor protein occurs at modest efficiency, the levels of functional receptors are low relative to those in eukaryotic cells (Jockers et al., 1994). However, our experiments failed to indicate that ligands supported receptor folding in bacteria.

When expression of the wild-type A_1 receptor in *E. coli* was induced in the presence of IBMX or DPCPX, the yield of wild-type receptor (140 ± 47 fmol/mg) was not altered; even the Y288A mutant was refractory to pharmacochaperoning in *E. coli* (Supplemental Fig. 2). Limited ligand diffusion was not the cause for ineffectiveness. To assess receptor accessibility we measured radioligand binding to intact bacterial cells. The data are plotted in Supplemental Fig. 2 inset, indicating that DPCPX bound specifically and with high affinity; no specific binding was found on noninduced bacteria (not shown). Thus, our data suggest that the biosynthesis in a eukaryotic cell is a necessary condition for pharmacochaperoning; the associated quality control exaggerates the folding deficiency. In bacterial membranes, the expression level of the Y288A mutant was approximately half the level of the wild-type receptor (Supplemental Fig. 2). Given the ratio observed in HEK293 cells (3/100; Fig. 1A) the relative expression level of the mutant receptor appeared more robust in bacteria.

Immunodetection of Receptor Isoforms. If gauged by antibody staining, pharmacochaperoning did not increase the amount of receptors in HEK293 cells. Figure 5A shows an immunoblot of the receptor protein immunoprecipitated from a cell lysate; as shown in Fig. 5B, receptors were precipitated with 10% trichloroacetic acid from combined density gradient fractions.

The immunblot in Fig. 5A shows two specific immunoreactive bands (both bands were absent in an immunoprecipitate from untransfected cells); the band at ~37 kDa likely represents the monomeric receptor protein, and the band at ~50 kDa may be a receptor concatemer or aggregate. After pharmacochaperoning (Fig. 5A, +), both bands arose from a single species. In untreated cells, however, the bands appeared wider, likely because they arose from a doublet band. The upper half of the wide bands may represent the mature form corresponding in size to the bands on the + lane in Fig. 5A, the lower half an immature form. Although not increasing the amount of receptor protein, pharmacochaperoning caused a shift in the apparent molecular mass of the receptor protein.

Likewise, after fractionation of cells expressing the YFP-tagged Y288A receptor (calculated molecular mass, ~64,000) light membranes (collected at "low" density; specific gravity, ~1.08–1.12 g/ml) comprised markedly more of the larger

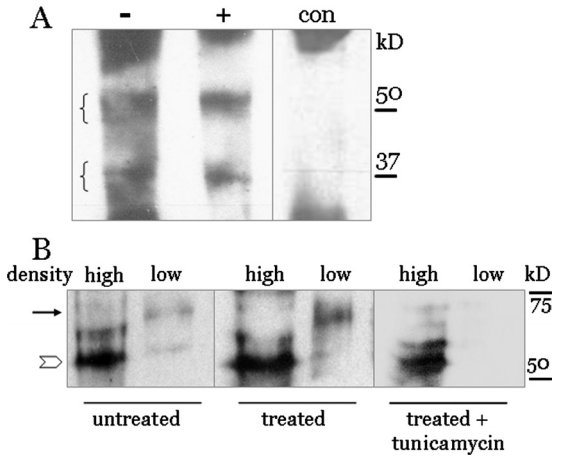

Fig. 5. Assessing the effect of pharmacochaperoning by immunoblot. A, membranes from HEK293 cells transfected with the HA-tagged mutant Y288A receptor that had been preincubated with 1 μM DPCPX (+) or vehicle (−) were solubilized and subjected to IP by using a mouse monoclonal anti-HA antibody. As control (con), membranes from nontransfected cells were used. The immunoblot was developed with anti-HA-antibody (polyclonal and monoclonal, mixed together); shown is the region bounded by nonspecific stains of IgG heavy and light chains. The brackets delineate the width of the receptor-specific stains. B, a postnuclear homogenate of HEK293 cells transfected with a YFP-tagged A_1R Y288A was fractionated on a sucrose gradient (as in the experiment in Fig. 4). Fractions with high density (approximately 1.13–1.15 g/ml specific gravity, containing ER membranes) and those with low density (approximately 1.08–1.12 g/ml, with plasma membranes) were combined, and protein was precipitated with trichloroacetic acid. An aliquot of the material was resolved on a urea-SDS gel. The immunoblot was developed by using anti-GFP and anti-FLAG antibodies mixed together. Cells had been incubated with 1 μM DPCPX or vehicle for 24 h; 2 μg/ml tunicamycin had been added for 15 h, as indicated. Arrow indicates the mature form of the receptor; arrowhead indicates the immature form.

protein band than did membranes from untreated cells. The combined fractions with high sucrose concentration ("high" density; specific gravity, ~1.13–1.15 g/ml) showed two smaller protein bands presumably corresponding to immature forms. Thus, addition of the chaperone did not markedly impinge on the overall receptor level but appeared to accelerate post-translational receptor maturation (through complex glycosylation, palmitoylation), increasing the amount of receptor bound to the light plasma membrane.

To confirm that the band shift was a corollary of receptor maturation, we incubated cells with tunicamycin (for 15 h before harvest), an inhibitor of GlcNAc phosphotransferase, required for the first step in protein glycosylation. In spite of coincubation with the chaperone ligand, the tunicamycin-treated cells were void of receptor immunoreactivity in the low-density fraction (Fig. 5B, right); however, receptor bands were detected in the heavier fraction, asserting the presence of a nonglycosylated folding intermediate.

Folding Intermediates that Bind Ligand Are Present in the ER. Our hypothesis therefore was that ligand binding assisted maturation and export by stabilizing a late folding intermediate. This had to be validated by demonstrating the presence of specific [^{3}H]DPCPX binding sites in ER membranes. The fractionation experiments shown in Fig. 4, however, failed to demonstrate radioligand binding to receptors retained in the ER. Even when transit was blocked with BFA there was no increase in binding sites that partitioned with ER-rich fractions (Fig. 4C). The use of BFA, however, might have introduced an experimental bias; we noticed a deleterious effect of BFA on cells overexpressing the receptor protein and reasoned that cells with a high level of retained receptors were particularly vulnerable to BFA, because of ER stress (Citterio et al., 2008).

We therefore resorted to transient transfection with a Sar1A mutant. Sar1A[T39N] (dnSar1A) is locked in the GDP-bound state. By sequestering the respective guanine nucleotide exchange factor (Sec12) dnSar1A suppresses the function of endogenous Sar1A in a dominant negative fashion (Kuge et al., 1994); in dnSar1A-transfected cells the recruitment of client molecules by coat protein complex II coat components is diminished. However, the block was not complete. Cotransfection with dnSar1A lowered the number of receptors detected by radioligand binding. Wild-type receptors were reduced by half (from 6.6 ± 0.8 to 3.6 ± 0.5 pmol/mg), and the F295A mutant was reduced to one-third the level in the controls (from 260 ± 75 to 80 ± 15 fmol/mg, three

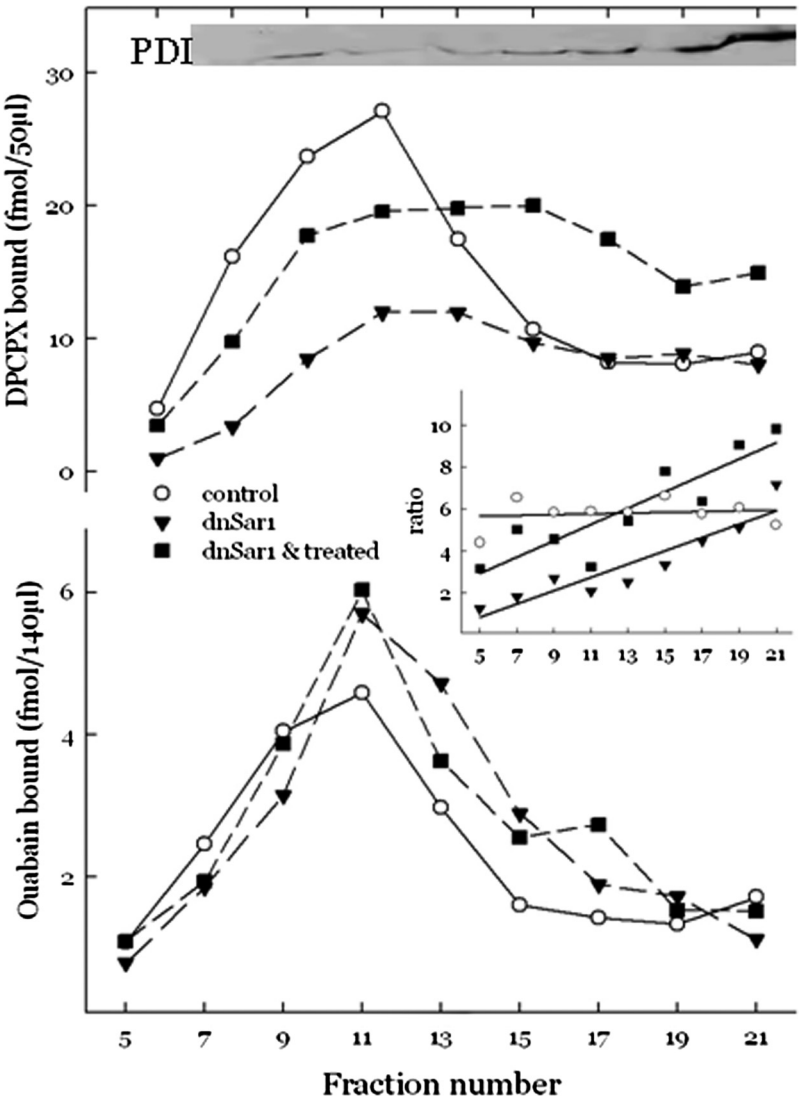

Fig. 6. Effect of a general ER export block on the subcellular distribution of ligand binding A_1 receptors. Top, fractionation of HEK293 cells transfected with wt A_1R plus Sar1A[T39N]. Fractionation and analysis of a post-nuclear supernatant from HEK293 cell homogenates was performed as in Fig. 4. A_1 receptor (top) and Na^+/K^+-ATPase-bound radioligand (bottom) are plotted as mol/fraction volume to document the fractionwise receptor recovery. Cells had been transfected with wt A_1R plus a control plasmid (○) or wt A_1R plus Sar1A[T39N] and incubated in the absence (■) or presence of DPCPX (▼). Inset, ratio of the specific binding values of [^{3}H]DPCPX over those of [^{3}H]ouabain.

transfection experiments each), indicating that they were indistinguishable in client recruitment at the ER exit site. In line with previous interpretations (Robert et al., 2005b; Thielen et al., 2005), this suggests that the proximal C-tail does not offer a docking site to the export machinery. The export block by dnSar1A was further exploited to demonstrate that ligand binding receptors could reside in the ER.

Figure 6 shows the distribution of radioligand binding (top: transiently transfected wt A_1R; bottom: endogenous Na^+/K^+-ATPase) in dnSar1A-transfected cells after fractionation on a density gradient (in an analogous manner to the fractionation shown in Fig. 4). In the control homogenate (cells transfected with wild-type receptor alone), the peaks of receptor and Na^+/K^+-ATPase binding activity coincided in fraction 11, which were, despite some overlap, set apart from the fractions containing PDI immunoreactivity (ER marker). In the presence of dnSar1A, however, the amount of radioligand bound decreased markedly, but the decrease was not equal among fractions. The receptor peak around fraction 11 was flatter than in the control; thus, the amount of A_1 receptor decreased in the light fractions (fractions 5–13, enriched in plasma membranes) but not in fractions of higher density, a finding indicative of reduced export. The distribution of Na^+/K^+-ATPase remained unchanged probably because of limited transfection efficiency (of dnSar1A).

Preincubation with DPCPX increased radioligand binding even in the presence of dnSar1A but receptors that bound radioligand were still kept in the ER; there was no change in the subcellular receptor distribution. This became evident from plotting the ratio of bound DPCPX to bound ouabain (Fig. 6, inset). The ratio was invariably the same if dnSar1A was absent (in the control): receptor and Na^+/K^+-ATPase colocalized. In the presence of dnSar1A, the ratio was low in the light fractions and increased along with fraction number; hence, the receptor was enriched, relative to Na^+/K^+-ATPase, in the dense fractions replete with ER membranes. Overexpressed wild-type receptors were previously demonstrated in the ER by immunoblot (Pankevych et al., 2003); here, we show that they were capable of ligand binding.

Pharmacochaperoning Accelerates Receptor Transfer to the Plasma Membrane via the Golgi Stacks. We predicted that, in the absence of a general export block, the preformed receptors exit swiftly once they are stabilized by a chaperone ligand. Thus, the onset of the pharmacochaperone effect should be faster than suggested by the radioligand binding experiment (shown in Fig. 3B); this was the case. We followed the fluorescent Y288A construct to estimate the pharmacochaperone-induced transfer rate (Fig. 7A). The distribution of the Y288A receptor before the addition of DPCPX is depicted in the first row of images in Fig. 7A. We found cells where the receptor showed nearly perfect overlay with the ER marker (in other instances receptor also colocalized with a Golgi marker, see below). When we added DPCPX, receptor redistribution occurred 1 h later. The receptor fluorescence accumulated in a 3- to 5-μm-wide region, which apparently did not colocalize with the ER but in the merge image exposed a bright, undimmed yellow stain. From 2 to 3 h on, the receptor depot became smaller, coinciding with the appearance of receptor fluorescence on the cell surface.

When we used a Golgi marker, it became obvious that the chaperone ligand released mutant receptors from the ER into

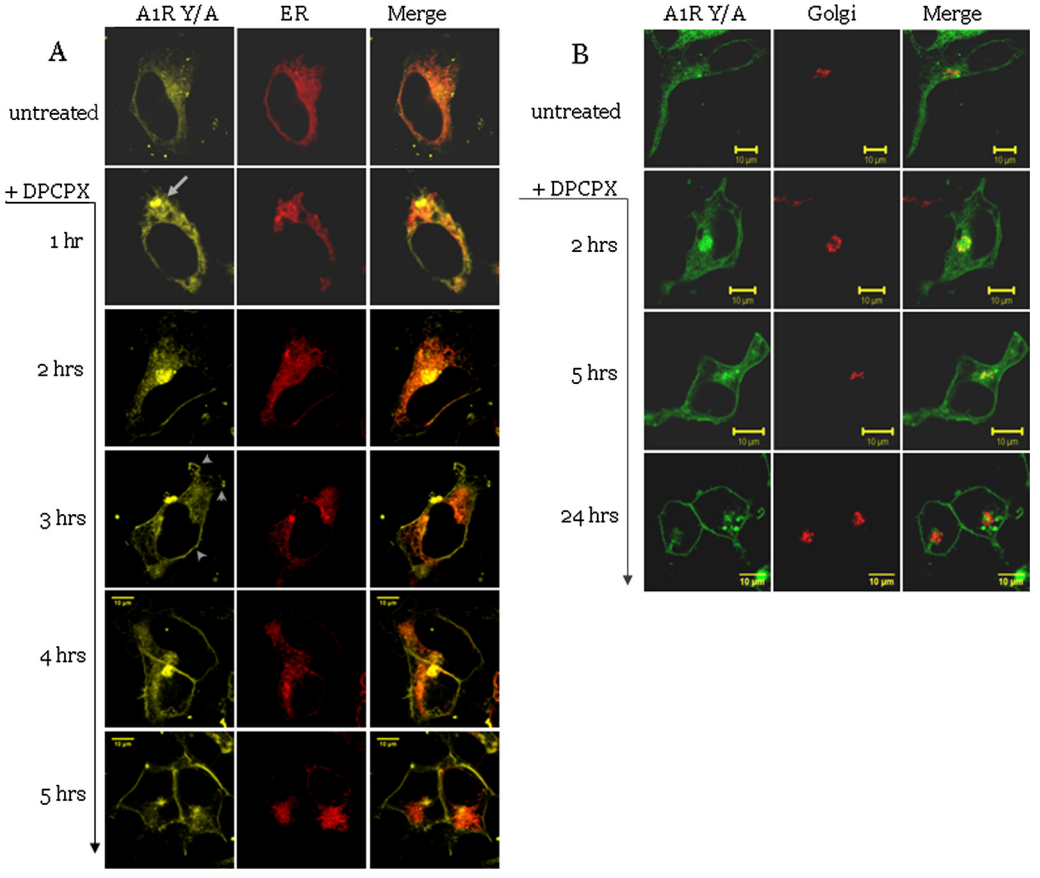

Fig. 7. Time course of A_1 receptor export followed by confocal microscopy. A, localization of A_1R Y288A (tagged with YFP and displayed in green) to the ER (CFP-tagged marker displayed in red) and time-dependent effect of the chaperone ligand. Images were captured at the indicated time points after the addition of 1 μM DPCPX. Arrowheads indicate membrane staining; the arrow points to an intracellular receptor depot filled after the addition of chaperone ligand. B, localization of A_1R Y288A (tagged with YFP and displayed green) to the Golgi cisternae (CFP-tagged marker represented in red) before and at several time points after the addition of DPCPX). Scale bar, 10 μm.

the Golgi stacks. Figure 7B demonstrates that receptor fluorescence localized to the Golgi 1 h after addition of DPCPX. In a typical example from untreated cells, as in the one shown in Fig. 7B, top, the Golgi fluorescence appeared offset from the fluorescence light emitted by the receptor. After the addition of DPCPX yellow dots were increasingly visible in the merge image. Colocalization was detected within an interval of up to 5 h. It almost vanished the next day when the receptor fluorescence was predominant on the cell borders.

Figure 8 provides for a quantitation of Y288A receptor redistribution by intensity correlation analysis (Li et al., 2004) where the extent of colocalization between receptor and the markers for ER (left) or Golgi (right) was evaluated. The principle is to compare CFP and YFP emission in each pixel of a double-fluorescent image. Given is the ICQ, which can vary between −0.5 and 0.5; values larger than zero indicate colocalization.

ICQ values from several images were averaged. Figure 8 gives the means from cells expressing A_1R Y288A together with ER marker (left) or Golgi marker (right); shown are the values from cells before and at two time points after the addition of DPCPX. The statistics confirm that retention of the mutant receptor was confined to the ER; smaller amounts were overlain with the Golgi marker. Addition of the chaperone ligand prompted redistribution from ER to the Golgi within 1 h. Further export decreased the amount of receptors retained in the ER and, consequently, receptor localization to the Golgi. The analysis of subcellular receptor redistribution demonstrated that escape from retention in the ER occurred without further delay. This is consistent with a stabilizing effect on preformed receptors.

Overexpression of DRiP78 Inhibits Export of the A_1 Adenosine Receptor. The Y288A and F295A mutations were designed to affect the structure of the proximal carboxyl terminus; the resulting disorder ought to be sensed by a chaperone molecule surveying the cytosolic domain. DRiP78, an Hsp40 family member, was reported to bind to the proximal C-tail of the D_1-dopamine receptor (Bermak et al., 2001), the sequence of which is related to that of the A_1 receptor (Table 1). DRiP78 is a putative membrane protein with two transmembrane spans, ER-retrieval sequences of the dilysine type, and a zinc-finger domain relevant for its binding to the receptor; its overexpression was shown to decrease the D_1-dopamine receptor level. We therefore tested whether the sequence similarity in the membrane-proximal C-tail is sufficient to provide for a similar regulation of the A_1 receptor.

Figure 9A shows the result of a co-IP experiment demonstrating physical interaction between the A_1 receptor (A_1R F295A, with an N-terminal HA tag) and DRiP78 (tagged on the C terminus with CFP). As in Bermak et al. (2001), we used a 5:1 transfection ratio (DRiP78 over receptor) to drive the interaction; membranes were prepared from transfected HEK293 cells and treated with a cross-linker (DSP) cleavable by reducing agents. After the IP of the receptor, the immunoblot was developed with an anti-HA and consecutively with an anti-GFP antibody. As control, a lysate was used from cells that had been transfected with DRiP78 alone (but no epitope-tagged receptor; Fig. 9A, lane con). A band corresponding to the receptor monomer was detected in the IP pellet (and a receptor concatemer; Fig. 9A, asterisk, lane transf) but not the control IP. Along with the receptor, a band corresponding to DRiP78 fused to CFP was detected with the anti-GFP antibody in the receptor IP pellet but not the control; the identity of the DRiP78-CFP (calculated molecular mass, ~105 kDa) band was confirmed by a single immunoreactive band in the input lysate that migrated to the same position.

We inferred from the report on the D_1 dopamine receptor (Bermak et al., 2001) that DRiP78 might similarly act to retain the A_1 receptor. We visualized CFP-tagged DRIP78 and a YFP-tagged mutant receptor in live cells. Confocal micrograph samples are shown in Fig. 9B (DRiP78 represented in red, receptor in green). The samples document ample overlay with the receptor, both before and after cell treatment with DPCPX. The images recorded after DPCPX treatment represent two types: one showing intense colocalization (bright merged yellow in rows 2 and 3 in Fig. 9B) and a second type where colocalization was less intense (dim yellow in rows 4 and 5 in Fig. 9B); the latter, but not the former, revealed membrane staining by the receptor YFP. Our impression was that the two types differed by the DRiP78 expression level. When the expression level was high, the receptor and DRiP78 appeared condensed in a circumscribed area (presumably delimited by the extension of the ER). With a lower DRiP78 level, however, the receptor transferred to the cell surface. Intracellular receptor retention despite incubation with a chaperone ligand was also documented by immunostaining of a CFP-less receptor (not shown). The impression conferred by the micrographs sug-

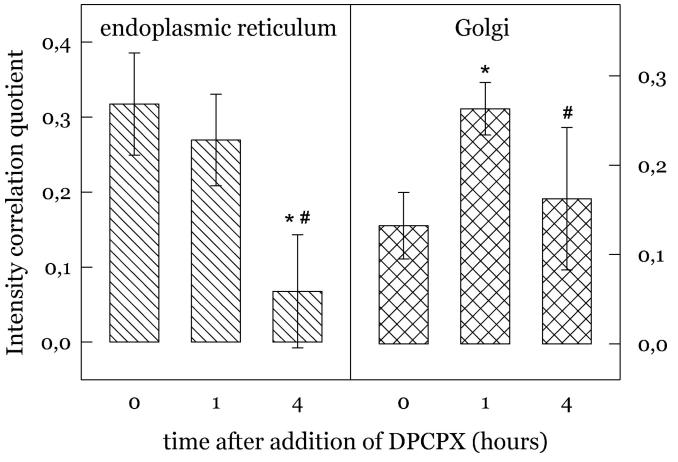

Fig. 8. Intensity correlation analysis for A_1R Y288A and the ER marker (left) or the Golgi marker (right). Given are the means (± S.D.) of the intensity correlation quotients from seven to 12 cells that have not been treated (0) or have been incubated for the indicated times with DPCPX. *, significant difference relative to value 0 h; #, significant difference relative to 1 h value ($p < 0.01$ determined by analysis of variance followed by Scheffé's post hoc comparison).

TABLE 1

Sequence alignment of the transmembrane α-helix 7–c-terminal tail (bold letters) junction of the indicated receptors (D_1 and D_2 dopamine, A_1 adenosine, and M_2 muscarinic)

The alignment highlights the pattern of equally spaced hydrophobic residues (underlined) proposed as the DRiP78-docking site (Bermak et al., 2001).

D1R	NPIIYA-F-**NADFQKAFSTLLGC**
A1R	NPIVYA-F**RIHKFRVTFLKIWND**
M2R	NPACYA-L**CNATFKKTFKHLLMC**
D2R	NPIIYTTF-**NIEFRKAFLKILHC**

gested that the amount of overexpressed DRiP78 determined the level of functional receptor. This was indeed the case. When we cotransfected DRiP78 and receptor at increasing ratios the density of receptors binding radioligand decreased accordingly.

Figure 10 gives the averaged results of DPCPX binding to membranes from cotransfected cells. Binding to the mutant receptors (A1R Y288A, F295A) decreased gradually; the decrease was significant at a 1:1 dose ratio but less so at a ratio of 0.5:1. Increasing the DRiP78 dose beyond the 2:1 ratio did not suppress the level of the mutant receptors further (not shown). It is noteworthy that there was a marked difference between the mutant and wild-type receptor in the amount of DRiP78 necessary to inhibit expression. At a dose ratio of 1:1 the mutant F295A and Y288A receptors dropped by ~50% but not the wild-type receptor, which required a 5-fold higher gene dose. All cells had been preincubated with IBMX for 24 h before harvest; therefore DRiP78, if overexpressed, antagonized rescue of the mutant receptors by pharmacochaperoning. These results support the conclusion that mutational lesions to the proximal C-tail resulted in receptor retention by an ER-resident chaperone molecule.

Discussion

In the present work, we substantiated the hypothesis that the structure of the proximal C-tail is critical for receptor export to the plasma membrane. Mutation of either the tyrosine or phenylalanine of the NPxxY(x)$_{5,6}$F sequence, which provide a link between the proximal C-tail and helix 7, caused intracellular retention of the A_1 receptor. However, the mutations would not create a major folding aberration (the alanine substitutions are compatible with helical secondary structures) and the mutant receptors proved to be functional; the deficiency appeared to be exaggerated by the quality-control system. Thus, the mammalian quality control was essential for judging the folding problem and similarly for pharmacochaperoning; neither one could be reproduced when the receptor was expressed in bacteria.

The site of retention of the mutant A_1 receptors, hence the site of pharmacochaperone action, was largely within bounds of the ER as suggested by the following evidence. 1) The retained receptor colocalized with an ER marker. 2) Addition of a chaperone ligand prompted receptor transfer to and accumulation in the Golgi. 3) BFA (an inhibitor of Golgi transit) and tunicamycin (an inhibitor of protein glycosylation) inhibited chaperone-prompted export. 4) Overexpression of the ER-associated Hsp40 protein DRiP78 led to retention through physical interaction with the receptor. However, a lesser proportion of mutant receptors spontaneously reached distal compartments of the secretory pathway including the Golgi stacks (see Fig. 7) and the plasma membrane. This is in agreement with the assumption that the folding defect was minor and fits the interpretation that the

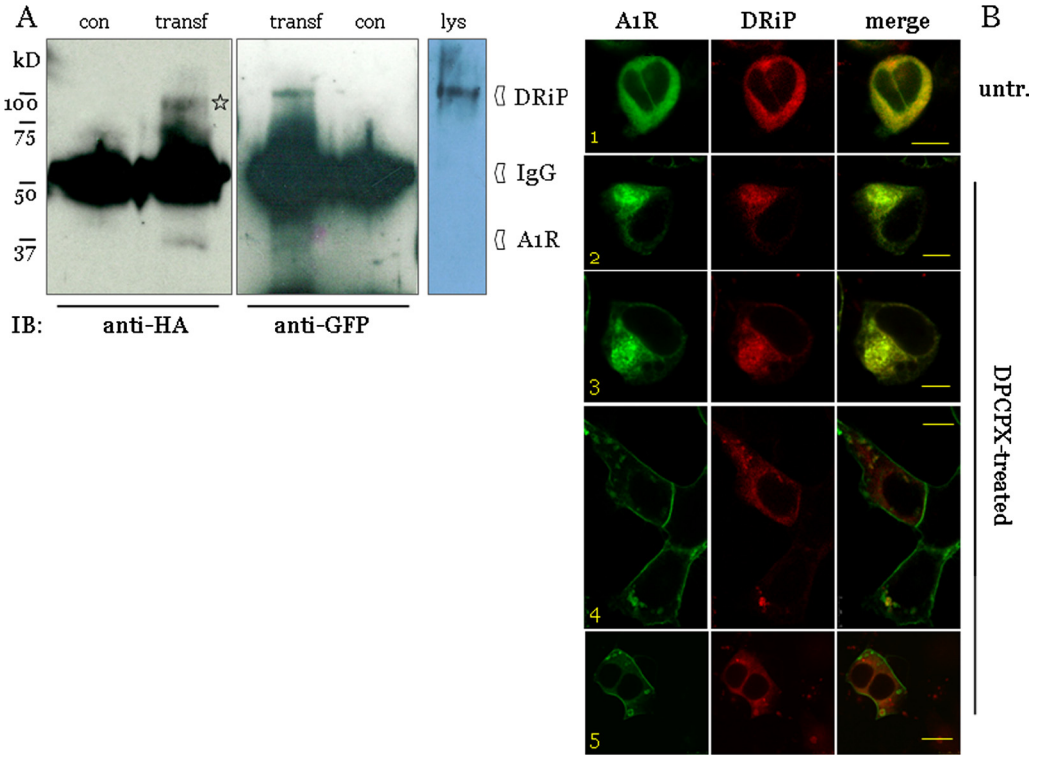

Fig. 9. Overexpressed DRiP78 binds to the mutant A_1 receptor and impinges on receptor localization. A, co-IP of the A_1 receptor (A_1R F295A) and DRiP78-CFP. A membrane preparation of HEK293 cells transfected with the receptor and DRiP78 (transf) constructs was treated with the chemical cross-linker DSP and solubilized. The receptor was precipitated with an anti-HA antibody; the immunoblot was sequentially developed with an anti-HA and an anti-GFP antibody to visualize receptor and DRiP78, respectively. Control cells were transfected with DRiP78-CFP alone (con). The asterisk indicates the position of an additional band immunoreactive to the anti-HA antibody (presumably a receptor concatemer). In the lys lane, the DRiP78-CFP band was visualized in the concentrated soluble supernatant by using an anti-GFP antibody and aligned according to the position of molecular mass markers. The experiment has been repeated with a similar result. B, colocalization of A_1R Y288A tagged with YFP (left, green) and DRiP78-CFP (center, red) in HEK293 cells cotransfected with equal amounts of either expression vector; overlaid images are shown (right). Numbers are row numbers. Untr., not treated with the chaperone ligand; DPCPX treatment was for 24 h before fixation. Representative confocal images recorded with 64× magnification and variable electronic zooms are shown. Scale bar, 10 μm.

chaperone ligand stabilized a distinct export-competent conformation the mutant receptors, as opposed to the wild type, failed to adopt spontaneously.

Our findings with the A_1 receptor support the current concept on pharmacochaperoning of G protein-coupled receptors. Chaperoning follows ligand binding to newly synthesized receptors at the site of biosynthesis (Petäjä-Repo et al., 2002, Wüller et al., 2004). Homosteric binding was demonstrated by the concentration-dependent effect of xanthine ligands with low and high affinity for the A_1 receptor. Either a specific antagonist or agonist ligand was efficient at chaperoning the mutant A_1 receptor; combining agonist with antagonist at saturating concentrations did not enhance or mitigate the effect (not shown). Thus, the occupancy of the ligand binding pocket rather than the receptor activity state causes the chaperone effect. This is in agreement with the conditions observed for chaperoning opioid receptors (Petäjä-Repo et al., 2002, Chaipatikul et al., 2003) or the H_2 histamine receptor (Alewijnse et al., 2000).

We further differentiated between early and late folding stages as targets for the chaperone ligand. The following observations argue against a model where the chaperone ligand induces the folding process ab initio (by the way of a folding nucleus). 1) When assessed by antibody staining, the amount of receptor protein did not increase after incubation with chaperone ligand. 2) The rate of receptor transfer from ER to Golgi had a rapid onset, rather compatible with an effect on preformed receptors. 3) In bacteria, there was no effect on the receptor number. Our findings therefore support the concept that the chaperone ligand has to bind to preformed receptors in the ER. Ligand binding likely induces a conformational change upon which the receptor protein transforms to the export-competent state and acquires the high-affinity binding state typical of the membrane-bound species. This is consistent with these observations. First, the chaperoning potency of DPCPX (EC_{50}, ~15 nM) was somewhat lower than its affinity for the surface-bound receptor (K_D for A_1R Y288A, ~1.2 ± 0.4 nM; not shown), and second, receptor species capable of binding ligand was scarce in the ER, because retained receptors exited once ligand occupancy had induced and stabilized the proper fold. Subcellular fractionation, in conjunction with the results from locating the receptor under the microscope (Figs. 1 and 4), demonstrated that ligand binding receptors predominantly resided in the plasma membrane but not within the cell (compare Pankevych et al., 2003). Conversely, it took a general export block to detect a substantial amount of bound radioligand in the ER (Fig. 6; compare Leskelä et al., 2007).

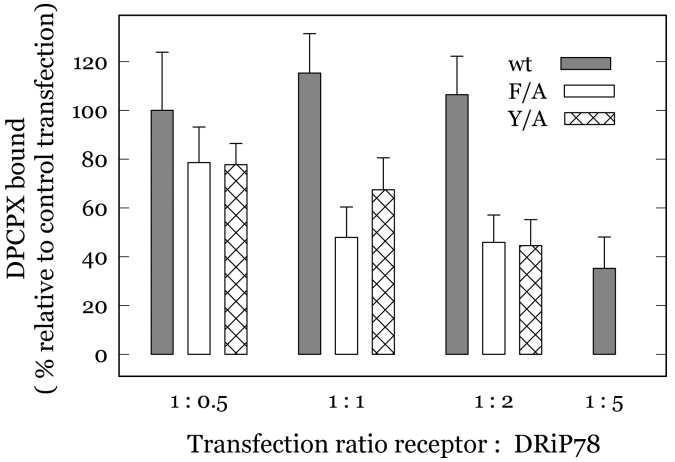

Fig. 10. DRiP78 suppresses the receptor binding level. [^{3}H]DPCPX binding to wt A_1R (filled bar), A_1R F295A (open bar), and A_1R Y288A (hatched bar) was determined in membranes from cells transfected with the receptor and DRiP78. The amount of DRiP78 plasmid was varied relative to the amount of receptor cDNA, the total amount of DNA being kept constant. In the control experiment, an empty vector substituted for the DRiP78 expression vector. The results were repeated with different total amounts of DNA (varying between 1 and 5 μg/dish). All cells were treated with 50 μM IBMX for 24 h before harvest. Binding values are expressed as percentage of the control (receptor + empty vector) transfection carried out in parallel. Each transfection experiment was performed at least three times; given are the means ± S.E.M.

We further suggest that the mutations of the $Y(x)_6F$ sequence resulted in an increased association with an ER resident component that held the receptor in the cell interior. The lectin-like proteins, although they bind to a G protein-coupled receptor as long as it is present in the ER (Morello et al., 2001; Mizrachi and Segaloff, 2004; Fan et al., 2005; Robert et al., 2005b; Leskelä et al., 2007; Duvernay et al., 2009), probably are not involved. The luminal lectin-like proteins cannot specifically recognize a membrane protein with a lesioned cytosolic or transmembrane domain (Kanehara et al., 2007).

Our candidate is a member of the Hsp40 protein family of molecular chaperones (Qiu et al., 2006). As paradigm example, we have tested DRiP78, which had been shown to associate to ER membranes and retain the D_1-dopamine and M_2-muscarinic (Bermak et al., 2001) receptors. We here add the A_1-adenosine and the D_2-dopamine receptors (C. Löwer and C. Nanoff, unpublished observation) to the list of DRiP78 substrates. These receptors have in common the reported DRiP78-recognition sequence [$F/L(x)_{3,4}FxxxF$] contained within the proximal C-tail (Table 1). In agreement with the report by Bermak et al. the inhibitory effect on the receptor level required relative overexpression of DRiP78; compared with the wild-type receptor the single-point mutants proved more susceptible to inhibition by DRiP78. It is thus attractive to speculate that DRiP78 can monitor and distinguish the faulty from the correct fold of the proximal C terminus. However, we cannot rule out that replacing the Y and F residues from the $Y(x)_6F$ sequence also impairs the stability of the transmembrane domain.

Mutations of the $NPxxY(x)_6F$ sequence may affect other intramolecular connections in addition to the one established by the tyrosine and phenylalanine side chains (Thielen et al., 2005; Urizar et al., 2005; Delos Santos et al., 2006). Molecular modeling, for example, suggested that the phenylalanine side chain interacts with a hydrophobic residue in α-helix 1 (Duvernay et al., 2009). The NPxxY sequence is known to form part of a network of inter-residue links between the transmembrane α-helices. Adaptation of the network to an altered $Y(x)_{5,6}F$ sequence, in fact, has been found to impinge on the configuration of the receptor transmembrane domain (Prioleau et al., 2002; Fritze et al., 2003). Our experimental evidence suggests that the Tyr288 and Phe295 mutations affected the transmembrane domain of the A_1 receptor. First, the chaperone effect occurred upon binding of either agonist or antagonist, irrespectively of the selected receptor conformation. Occupancy of the binding pocket was sufficient, presumably by stabilizing the transmembrane domain (helix 8 does not contribute to the binding pocket). Second, a double-

mutant receptor (Y288A/F295A), whose expression level was below detection, weakly responded to xanthine antagonists; the extent of rescue was modest by the high-affinity ligand DPCPX, whereas IBMX was entirely ineffective (data not shown), findings similar to a receptor construct that lacked the entire C-tail (Hawtin, 2006). This confirms that the Tyr288 and Phe295 residues have additional connections that extend to the ligand binding pocket. In line with this assumption, the mutant receptors differed by the ability to form a ternary high-affinity complex (increased in the untreated F295A mutant, decreased in the Y288A mutant); either mutation had a specific, but dissimilar, consequence on G protein coupling, hence on the conformation of the activated receptor.

It thus appears possible that the proximal carboxyl terminus contributes to the compactness of transmembrane receptor domain, accounting for the fact that helix 8 was the only cytoplasmic segment uniformly defined by the available receptor crystal structures (e.g., Cherezov et al., 2007). As parsimonious interpretation, we suggest that the effect of the chaperone ligand is caused by stabilizing the transmembrane structure including helix 8; this leads to the dissociation of an Hsp40 protein (such as DRiP78) and efficient receptor export.

References

Alewijnse AE, Timmerman H, Jacobs EH, Smit MJ, Roovers E, Cotecchia S, and Leurs R (2000) The effect of mutations in the DRY motif on the constitutive activity and structural instability of the histamine H(2) receptor. *Mol Pharmacol* **57:**890–898.

Bermak JC, Li M, Bullock C, and Zhou QY (2001) Regulation of transport of the dopamine D1 receptor by a new membrane-associated ER protein. *Nat Cell Biol* **3:**492–498.

Chaipatikul V, Erickson-Herbrandson LJ, Loh HH, and Law PY (2003) Rescuing the traffic-deficient mutants of rat μ-opioid receptors with hydrophobic ligands. *Mol Pharmacol* **64:**32–41.

Cherezov V, Rosenbaum DM, Hanson MA, Rasmussen SG, Thian FS, Kobilka TS, Choi HJ, Kuhn P, Weis WI, Kobilka BK, et al. (2007) High-resolution crystal structure of an engineered human β2-adrenergic G protein-coupled receptor. *Science* **318:**1258–1265.

Citterio C, Vichi A, Pacheco-Rodriguez G, Aponte AM, Moss J, and Vaughan M (2008) Unfolded protein response and cell death after depletion of brefeldin A-inhibited guanine nucleotide-exchange protein GBF1 *Proc Natl Acad Sci USA* **105:** 2877–2882.

Conn PM, Knollman PE, Brothers SP, and Janovick JA (2006) Protein folding as posttranslational regulation: evolution of a mechanism for controlled plasma membrane expression of a G protein-coupled receptor. *Mol Endocrinol* **20:**3035–3041.

Delos Santos NM, Gardner LA, White SW, and Bahouth SW (2006) Characterization of the residues in helix 8 of the human β1-adrenergic receptor that are involved in coupling the receptor to G proteins. *J Biol Chem* **281:**12896–12907.

Duvernay MT, Zhou F, and Wu G (2004) A conserved motif for the transport of G protein-coupled receptors from the endoplasmic reticulum to the cell surface. *J Biol Chem* **279:**30741–30750.

Duvernay MT, Dong C, Zhang X, Zhou F, Nichols CD, and Wu G (2009) Anterograde trafficking of G protein-coupled receptors: function of the C-terminal F(X)6LL motif in export from the endoplasmic reticulum. *Mol Pharmacol* **75:**751–761.

Fan J, Perry SJ, Gao Y, Schwarz DA, and Maki RA (2005) A point mutation in the human melanin concentrating hormone receptor 1 reveals an important domain for cellular trafficking. *Mol Endocrinol* **19:**2579–2590.

Fritze O, Filipek S, Kuksa V, Palczewski K, Hofmann KP, and Ernst OP (2003) Role of the conserved NPxxY(x)5,6F motif in the rhodopsin ground state and during activation. *Proc Natl Acad Sci USA* **100:**2290–2295.

Gáborik Z, Mihalik B, Jayadev S, Jagadeesh G, Catt KJ, and Hunyady L (1998) Requirement of membrane-proximal amino acids in the carboxyl-terminal tail for expression of the rat AT1a angiotensin receptor. *FEBS Lett* **428:**147–151.

Hawtin SR (2006) Pharmacological chaperone activity of SR49059 to functionally recover misfolded mutations of the vasopressin V1a receptor. *J Biol Chem* **281:** 14604–14614.

Huyer G, Piluek WF, Fansler Z, Kreft SG, Hochstrasser M, Brodsky JL, and Michaelis S (2004) Distinct machinery is required in *Saccharomyces cerevisiae* for the endoplasmic reticulum-associated degradation of a multispanning membrane protein and a soluble luminal protein. *J Biol Chem* **279:**38369–38378.

Jockers R, Linder ME, Hohenegger M, Nanoff C, Bertin B, Strosberg AD, Marullo S, and Freissmuth M (1994) Species difference in the G protein selectivity of the human and bovine A1 adenosine receptor. *J Biol Chem* **269:**32077–32084.

Kanehara K, Kawaguchi S, and Ng DT (2007) The EDEM and Yos9p families of lectin-like ERAD factors. *Semin Cell Dev Biol* **18:**743–750.

Klinger M, Freissmuth M, and Nanoff C (2002) Adenosine receptors: G protein-mediated signalling and the role of accessory proteins. *Cell Signal* **14:**99–108.

Kuge O, Dascher C, Orci L, Rowe T, Amherdt M, Plutner H, Ravazzola M, Tanigawa G, Rothman JE, and Balch WE (1994) Sar1 promotes vesicle budding from the endoplasmic reticulum but not Golgi compartments. *J Cell Biol* **125:**51–65.

Leskelä TT, Markkanen PM, Pietilä EM, Tuusa JT, and Petäjä-Repo UE (2007) Opioid receptor pharmacological chaperones act by binding and stabilizing newly synthesized receptors in the endoplasmic reticulum. *J Biol Chem* **282:**23171–23183.

Li Q, Lau A, Morris TJ, Guo L, Fordyce CB, and Stanley EF (2004) A syntaxin 1, Gα(o), and N-type calcium channel complex at a presynaptic nerve terminal: analysis by quantitative immunocolocalization. *J Neurosci* **24:**4070–4081.

Mizrachi D and Segaloff DL (2004) Intracellularly located misfolded glycoprotein hormone receptors associate with different chaperone proteins than their cognate wild-type receptors. *Mol Endocrinol* **18:**1768–1777.

Morello JP, Salahpour A, Laperrière A, Bernier V, Arthus MF, Lonergan M, Petäjä-Repo U, Angers S, Morin D, Bichet DG, et al. (2000) Pharmacological chaperones rescue cell-surface expression and function of misfolded V2 vasopressin receptor mutants. *J Clin Invest* **105:**887–895.

Morello JP, Salahpour A, Petäjä-Repo UE, Laperrière A, Lonergan M, Arthus MF, Nabi IR, Bichet DG, and Bouvier M (2001) Association of calnexin with wild type and mutant AVPR2 that causes nephrogenic diabetes insipidus. *Biochemistry* **40:**6766–6775.

Noorwez SM, Kuksa V, Imanishi Y, Zhu L, Filipek S, Palczewski K, and Kaushal S (2003) Pharmacological chaperone-mediated in vivo folding and stabilization of the P23H-opsin mutant associated with autosomal dominant retinitis pigmentosa. *J Biol Chem* **278:**14442–14450.

Oksche A, Dehe M, Schülein R, Wiesner B, and Rosenthal W (1998) Folding and cell surface expression of the vasopressin V2 receptor: requirement of the intracellular C-terminus. *FEBS Lett* **424:**57–62.

Pankevych H, Korkhov V, Freissmuth M, and Nanoff C (2003) Truncation of the A1 adenosine receptor reveals distinct roles of the membrane-proximal carboxyl terminus in receptor folding and G protein coupling. *J Biol Chem* **278:**30283–30293.

Petäjä-Repo UE, Hogue M, Bhalla S, Laperrière A, Morello JP, and Bouvier M (2002) Ligands act as pharmacological chaperones and increase the efficiency of delta opioid receptor maturation. *EMBO J* **21:**1628–1637.

Plagemann PG and Wohlhueter RM (1984) Inhibition of the transport of adenosine, other nucleosides, and hypoxanthine in novikoff rat hepatoma cells by methylxanthines, papaverine, N^6-cyclohexyladenosine and N^6-phenylisopropyladenosine. *Biochem Pharmacol* **33:**1783–1788.

Prioleau C, Visiers I, Ebersole BJ, Weinstein H, and Sealfon SC (2002) Conserved helix 7 tyrosine acts as a multistate conformational switch in the 5HT2C receptor. Identification of a novel "locked-on" phenotype and double revertant mutations. *J Biol Chem* **277:**36577–36584.

Qiu XB, Shao YM, Miao S, and Wang L (2006) The diversity of the DnaJ/Hsp40 family, the crucial partners for Hsp70 chaperones. *Cell Mol Life Sci* **63:**2560–2570.

Robert J, Clauser E, Petit PX, and Ventura MA (2005a) A novel C-terminal motif is necessary for the export of the vasopressin V1b/V3 receptor to the plasma membrane. *J Biol Chem* **280:**2300–2308.

Robert J, Auzan C, Ventura MA, and Clauser E (2005b) Mechanisms of cell-surface rerouting of an endoplasmic reticulum-retained mutant of the vasopressin V1b/V3 receptor by a pharmacological chaperone. *J Biol Chem* **280:**42198–42206.

Sawyer GW, Ehlert FJ, and Shults CA (2010) A conserved motif in the membrane proximal C-terminal tail of human muscarinic m1 acetylcholine receptors affects plasma membrane expression. *J Pharmacol Exp Ther* **332:**76–86.

Thielen A, Oueslati M, Hermosilla R, Krause G, Oksche A, Rosenthal W, and Schülein R (2005) The hydrophobic amino acid residues in the membrane-proximal C tail of the G protein-coupled vasopressin V2 receptor are necessary for transport-competent receptor folding. *FEBS Lett* **579:**5227–5235.

Urizar E, Claeysen S, Deupí X, Govaerts C, Costagliola S, Vassart G, and Pardo L (2005) An activation switch in the rhodopsin family of G protein-coupled receptors: the thyrotropin receptor. *J Biol Chem* **280:**17135–17141.

Van Craenenbroeck K, Clark SD, Cox MJ, Oak JN, Liu F, and Van Tol HH (2005) Folding efficiency is rate-limiting in dopamine D4 receptor biogenesis. *J Biol Chem* **280:**19350–19357.

Wüller S, Wiesner B, Löffler A, Furkert J, Krause G, Hermosilla R, Schaefer M, Schülein R, Rosenthal W, and Oksche A (2004) Pharmacochaperones post-translationally enhance cell surface expression by increasing conformational stability of wild-type and mutant vasopressin V2 receptors. *J Biol Chem* **279:**47254–47263.

Address correspondence to: Christian Nanoff, Institute of Pharmacology, Medizinische Universität Wien, Währinger Strasse 13A, 1090 Wien, Austria. E-mail: christian.nanoff@meduniwien.ac.at